Research Square

Preprints are preliminary reports that have not undergone peer review.
They should not be considered conclusive, used to inform clinical practice,
or referenced by the media as validated information.

MicroRNA-22-3p is associated with spinal cord injury regeneration and PTEN/STAT3 signaling

Sevil Köse
Akdeniz University
Ömer Özkan
Akdeniz University
Seval Tanrıkulu Kirişçi
Akdeniz University
Onural Tümer
Akdeniz University
Ebru Apaydın Doğan
Akdeniz University
Özlenen Özkan
ozlenenozkan@akdeniz.edu.tr
Akdeniz University

Research Article

Keywords: Spinal cord injury, SCI, miR-22, motor activity, cell survival

Posted Date: November 12th, 2026

DOI: https://doi.org/10.21203/rs.3.rs-11219023/v1

License: This work is licensed under a Creative Commons Attribution 4.0 International License.
Read Full License

Additional Declarations: No competing interests reported.

MicroRNA-22-3p is associated with spinal cord injury regeneration and PTEN/STAT3 signaling

Sevil KÖSE[1], Ömer ÖZKAN[1], Seval TANRIKULU KİRİŞÇİ1, Onural TÜMER[2], Ebru APAYDIN DOĞAN[2], Özlenen ÖZKAN[1]*

1Department of Plastic, Reconstructive and Aesthetic Surgery, Faculty of Medicine, Akdeniz University, Antalya, Turkey

2Faculty of Medicine, Department of Neurology, Akdeniz University, Antalya, Turkey

*Correspondence author:

Prof. Dr. Özlenen Özkan

Department of Plastic, Reconstructive and Aesthetic Surgery, Faculty of Medicine, Akdeniz University, Antalya, Turkey

ozlenenozkan@akdeniz.edu.tr

Abstract

Spinal cord injury (SCI) is a debilitating condition with limited treatment options, where secondary injury mechanisms such as oxidative stress, cell death, and inflammation exacerbate tissue damage and impair recovery. MicroRNA-22 (miR-22) is recognized for its antioxidant, anti-inflammatory, and cell survival properties; however, its specific role in SCI remains unclear. This study aimed to investigate the effects of miR-22 modulation on neuronal survival and functional recovery in a rat model of SCI, with a particular focus on the PTEN/AKT and STAT3 signaling pathways. Following clip-compression induced SCI, rats were transfected with either a miR-22 mimic or an antagomir. Behavioral and electrophysiological assessments revealed that miR-22-overexpression improved motor recovery and proximal latency compared to the SCI-only and SCI + antagomir transfected groups. Histological analysis demonstrated enhanced neuronal survival in the miR-22 transfected group compared with the SCI and SCI + antagomir transfected groups. ELISA results showed reduced expression of the cell death markers Bcl-2 and Caspase-3. Furthermore, qRT-PCR analysis showed that miR-22 expression was downregulated following SCI and upregulated after miR-22 transfection. Elevated miR-22 levels were associated with reduced PTEN and STAT3 expression, partial restoration of CREB1 levels, while AKT mRNA expression remained unchanged. GFAP expression was increased after SCI but was not significantly affected by miR-22 treatment compared with the SCI group. Collectively, these findings suggest that miR-22 may be involved in neuroprotection and functional recovery following SCI and is associated with changes in PTEN- and STAT3-related signaling. Therefore, miR-22 may represent a potential therapeutic target for SCI, although further mechanistic and translational studies are required.

Keywords: Spinal cord injury, SCI, miR-22, motor activity, cell survival

Introduction

Spinal cord injury (SCI) is a devastating neurological disorder that results in the permanent loss of motor, sensory, and autonomic functions, severely compromising patients' quality of life [1]. According to the World Health Organization (WHO), between 250,000 to 500,000 people globally suffer from SCI each year [2]. Despite advancements in surgical and supportive care, no curative treatment currently exists. The pathophysiology of SCI is highly complex, beginning with a primary mechanical insult and progressing through secondary injury mechanisms-including oxidative stress, apoptosis, excitotoxicity, and chronic inflammation-which collectively exacerbate neuronal damage and impede functional recovery [3, 4]. Consequently, there is a pressing need to identify molecular targets that can promote neuroprotection and regeneration.

MicroRNAs (miRNAs) have emerged as critical post-transcriptional regulators of gene expression and are involved in diverse biological processes such as neuronal survival, plasticity, and repair [5]. Among them, microRNA-22 (miR-22) has demonstrated anti-oxidative, anti-inflammatory, and anti-apoptotic effects in neuronal and glial cells [6, 7]. It is broadly expressed in various body tissues, including the brain [8-10], and has been reported to be expressed in both neurons and glial cells [11]. Notably, miR-22 expression increases in spinal cord tissue following traumatic SCI in mice [12]. Experimental evidence studies suggest that miR-22 may modulate key signaling pathways relevant to SCI recovery, such as the PI3K/AKT and PTEN-mediated cascades, which are central to axonal regeneration and neuronal survival [13, 14]. However, the precise role of miR-22 in SCI remains largely unexplored, with only a few studies describing its post-injury expression dynamics and molecular mechanisms.

Based on this evidence, we hypothesize that miR-22 facilitates functional recovery after SCI by regulating cell survival pathways and promoting neuronal regeneration. This study

investigates the effects of modulating miR-22 in a rat model of SCI, focusing on functional recovery, histological outcomes, and the expression of cell survival and regeneration-related markers. By elucidating the molecular role of miR-22 in SCI pathophysiology, our work aims to provide novel insights into its potential as a therapeutic candidate for spinal cord repair.

Methods

We designed a prospective, randomized, controlled in vivo study. All animal procedures were approved by the Institutional Animal Care and Use Committee of Akdeniz University (Protocol Number #1564/2023.05.002). All experiments were carried out at the Animal Experiment Center of Akdeniz University, Turkey, with animals housed and handled in accordance with established guidelines for laboratory animal care. Compliance with the ARRIVE 2.0 guidelines [15], was ensured, and the ARRIVE checklist was utilized to provide comprehensive information on the experimental design, determination of sample size, randomization and blinding procedures, as well as steps taken to protect animal welfare. Animals were assigned to experimental groups by an independent observer, based on body weight, to ensure balanced distribution across groups. During the experimental days, animals were randomly selected by an animal care technician. All tests were performed in a blinded manner, and the animal codes were revealed only at the end of experiments.

Animals and treatment procedures

A total of 108 adult male Sprague Dawley rats (250–320 g; 8-10 weeks) were obtained from the Animal Center of Akdeniz University. The rats were housed under a 12:12- hour light-dark cycle with free access to food and water. The room temperature was maintained at 25 ± 3 °C with a relative humidity of 60 ± 15%. The animals were divided into 4 groups: the sham-operated control group rats underwent laminectomy without induction of spinal cord injury (SCI) and did not receive any other agent (Sham, n=27); control group rats underwent SCI after

laminectomy and were given the liposomal transfection agent without further treatment (SCI, n=27); miR-22-3p transfected group rats were given the miR-22-3p and liposomal transfection agent after laminectomy and SCI (SCI + miR-22, 100 nmol/ mL, n=27); miR-22 antagomir transfected group rats were given the mir-22 antagomir and liposomal transfection agents after laminectomy and SCI (SCI + anta-miR-22, 100 nmol/ mL, n=27) (Fig. 1A).

Surgical procedures were performed under anesthesia induced by an intraperitoneal injection of a ketamine/xylazine cocktail (87.5 mg/kg and 12.5 mg/kg, respectively). The rats were placed in a prone position and surgical site was shaved and disinfected. A laminectomy was performed at the T8-10 vertebrae to expose the spinal cord. A clip-compression model of injury was then induced using a pair of aneurysm clips (JOHNS-HOPKINS Bulldog Clamp, 38 mm). The clips were applied to pinch the dorsal spinal cord tissues between the bilateral dorsal roots, inserted to a depth of 2 mm, and maintained for 10 seconds [16]. Successful injury was confirmed by observable tail spasms, retraction-like leg flutters, and delayed paralysis. In the groups designated for transfection, transfection agents were administered to the injured area according to the groups, one minute after clip removal. One-minute post-administration, the surgical wound was closed in layers. At the predetermined time points outlined in the experimental design (Fig. 1A), the rats were euthanized via an overdose of ketamine (90 mg/kg, i.p.) and xylazine (10 mg/kg, i.p.). Subsequently, approximately 0.5 cm of spinal cord tissue centered on the injury site was harvested for analysis.

Transfection of microRNA mimic and antagomir

A synthetic miR-22-3p miRNA mimic (miR-22; ABM, # MCH01594) or miR-22 antagomir (anta-miR-22; ABM, #MNH01581) were mixed with a complexation buffer at 1:1 ratio. After 5 min, the mixture was combined with Invivofectamine 3.0 (# IVF3001, ThermoFisher) at a 1:1 volume ratio, vortexed for 30 s, and incubated at 50 °C for 30 min. The resulting solution was then diluted with PBS. All rats received a fixed dose of 0.5 nmol of either miR-22-3p or

the miR-22 antagomir, suspended in a total vehicle volume of 50 µL (5% Invivofectamine in PBS). The freshly prepared solution was kept at room temperature throughout the administration procedure [17].

Motor activity assessment

The rats were initially weighed on days 1, 7, 14, 21 and 28. Hindlimb motor function was evaluated using the 22-point (0-21) Basso, Beattie, and Bresnahan (BBB) open-field locomotor scale, which assesses joint movement, stepping ability, coordination, and trunk stability. A score of 21 indicates unimpaired locomotion, as observed in the sham-operated rats (Sham group). All animals underwent behavioral testing, with each session lasting 5 min. These evaluations were performed by two observers who were blinded to the treatment groups of the animals [18]. Motor performance was further assessed using the inclined plane test. In this test, rats were positioned lengthwise on a plane with an initial angle of 10°. The angle was then incrementally increased until the rat could maintain its position for 5 seconds. This procedure was repeated three times per animal, and the average angle was recorded as the motor score [19].

Hindlimb locomotor activity was also measured through footprint analysis. The soles of the rats' feet were coated with non-toxic black paint, and the animals were allowed to walk along a narrow, white paper-covered runway. At least 4–5 sequential steps were used to calculate the mean values for step width, step length, and toe spread. The measurements were obtained using ImageJ software (version 1.54 g, National Institutes of Health, USA) [20]. First, foot print images were converted to 8-bit grayscale. The threshold value was set at 153-214, determined based on preliminary analysis and kept constant for all analyses. All experiments were conducted on days 1, 7, 14, 21 and 28, with statistical analyses performed independently for each time point.

Electrophysiological evaluation

Electrophysiological measurements were performed four weeks after the study began. The animals were placed in a prone position with their hindlimbs fully extended. Two vertical incisions were made at the estimated levels of the stimulation zones. Electrophysiological measurements were taken using Neuropack M1 MEB-9200 device (Nihon-Kohden Corp, Tokyo, Japan). The rats were electrically stimulated with concentric needle electrodes at two different points in the spinal cord; the T6-7 and T11-12 spinal segments. Compound muscle action potentials (CMAPs) were recorded from the left gastrocnemius muscle by concentric needle electrodes, with the ground electrode placed on the base of tail. Electrical stimulation was delivered as a square pulse with a frequency of 1 Hz and a duration of 0.2 m/s. The stimulus current intensity was gradually increased to a supramaximal level (30% above the current required to evoke the maximal CMAP). Stimulation was repeated five times for all measurements, and the average values were recorded. The amplitudes, areas, onset latencies, and durations of CMAPs were evaluated. The spinal cord conduction velocity (SCCV) were calculated by analyzing the latency difference between the CMAPs.

Histological analysis

To evaluate the contusion area, neuronal density, and cavity formation, histological staining was conducted using Hematoxylin–eosin (HE; Merck, #1.09253 and #1.09844) and Cresyl violet (0.1%; Sigma-Aldrich, #C5042). Seven days post-surgery, rats were sacrificed, and the T8-11 spinal cord segments containing the lesion epicenter were harvested. Tissue samples (a 0.5 cm segment centered on the injury) were fixed in 4% formalin for 24 h, processed for paraffin embedding, and sectioned at 6 μm. Following deparaffinization in xylene and dehydration through a graded ethanol series, the sections were stained with HE [21] and Cresyl violet [22]. After a final dehydration and clearing steps, the sections were coverslipped with Entellan and visualized under a Zeiss Primovert optical microscope. Digital images were

acquired with an Axiocam system using Zen 3.3 software (Zeiss). Quantitative analysis was performed on five random fields from each of three slides per animal using ImageJ software [20]. Histological analysis images were converted to 8-bit grayscale. The threshold value was set at 153-214, determined based on preliminary analysis and kept constant for all analyses.

RNA isolation and quantitative real-time PCR

Total RNA was isolated using the Ecopure total RNA kit (Ecotech biotech, #E2075, Turkey) according to the manufacturer's instructions. For miRNA expression analysis, RNA was reverse-transcribed into complementary DNA (cDNA) using the miRNA All-In-One cDNA Synthesis Kit (ABM, #G898, Canada). Quantitative real-time PCR (qRT-PCR) was subsequently performed with A.B.T. 2X qPCR SYBR-Green MasterMix (#Q03-02-05, Turkey) on a CFX96 Real-Time PCR Detection System (Bio-Rad, USA). The relative expression levels and transfection efficiency were calculated using the 2-ΔΔCT method, with U6 small nuclear RNA (snRNA; MS00033740) serving as internal control [23],. The primer sequences used were as follows: U6, forward: 5′-GCTTCGGCAGCACATATACTAAAAT-3′, reverse: 5′-CGCTTCACGAATTTGCGTGTCAT-3′; miR-22-3p, forward: 5`-GTTCTTCAGTGGCAAGC-3`, reverse: 5`-GAACATGTCTGCGTATCTC-3`; B-actin, forward: TGGTGGGTATGGGTCAGAAG, reverse: GACAATGCCGTGTTCAATGG; PTEN, forward: TTGGCGGTGTCATAATGTCT, reverse: GCAGAAAGACTTGAAGGCGTA; STAT3, forward: AATATAGCCGATTCCTGCAAGAG, reverse: TGGCTTCTCAAGATACCTGCTC; AKT, forward: GTGGCAAGATGTGTATGAG, reverse: CTGGCTGAGTAGGAGAAC; CREB1, forward: CCAAACTAGCAGTGGGCAGTATATT, reverse: GGTACCATTGTTAGCCAGCTGTATT.

Enzyme-linked immune sorbent (ELISA) assay

The levels of rat Bcl-2 (#RE1063R), Caspase-3 (#RE2850R) and GFAP (#RE2813R) in spinal cord lysates were measured immunoenzymatically using commercially available kits (Reed Biotech, China), according to the manufacturer's instructions. The optical density (OD) for each sample was determined at 450 nm with a reference wavelength of using a microplate reader. The concentrations of Bcl-2, Caspase-3, and GFAP were calculated on a standard curve [24].

Statistical analysis

An a priori power analysis (powerandsamplesize.com) was conducted to determine the target sample size for the primary comparison, aiming for ≥80% power at α=0.05; this informed the planned group size for behavioral experiments (six per group) unless otherwise noted. Statistical analyses were performed using GraphPad Prism software (version 9.5.0). Normality was assessed using Shapiro–Wilk; homogeneity using Welch's ANOVA test. The results of the tests for normality and variance homogeneity reported for each experiment (in the supplement). Kruskal-Wallis test and Dunn's multiple comparisons tests were performed for nonparametric data and one-way ANOVA and Tukey's multiple comparisons test were performed for parametric data. Longitudinal data in the same biological replicates compared using repeated measures (RM) one-way ANOVA test with Geisser-Greenhouse correction and Tukey's multiple comparisons test. Nonparametric data displayed as median and interquartile range (in the supplement). A p-value of less than 0.05 was considered statistically significant.

Results

The number of Nissl-positive cells in the miR-22–transfected animals was higher than that in the SCI-only group

We evaluated the effects of miR-22 transfection on spinal cord tissue by assessing contusion area, neuronal density, and cavity formation. Histograms (Fig. 1B) and histological analysis (Fig. 1C, Table S1) revealed that the number of Nissl positive cells is higher in the miR-22

transfected group (SCI + miR-22) compared to SCI + anta-miR-22 group ($p=0.0189$). The number of cells obtained from the sections of Sham group was higher compared to the SCI ($p=0.0189$) and SCI + anta-miR-22 ($p<0.0001$) groups (Fig. 1B, C; Table S1). Analysis of the cavity areas on the slides revealed that the Sham group had a smaller lacunar area compared to SCI ($p=0.0321$), SCI + miR-22 ($p=0.0004$) and SCI + anta-miR-22 groups ($p=0.0004$) (Fig. 1D; Table S1).

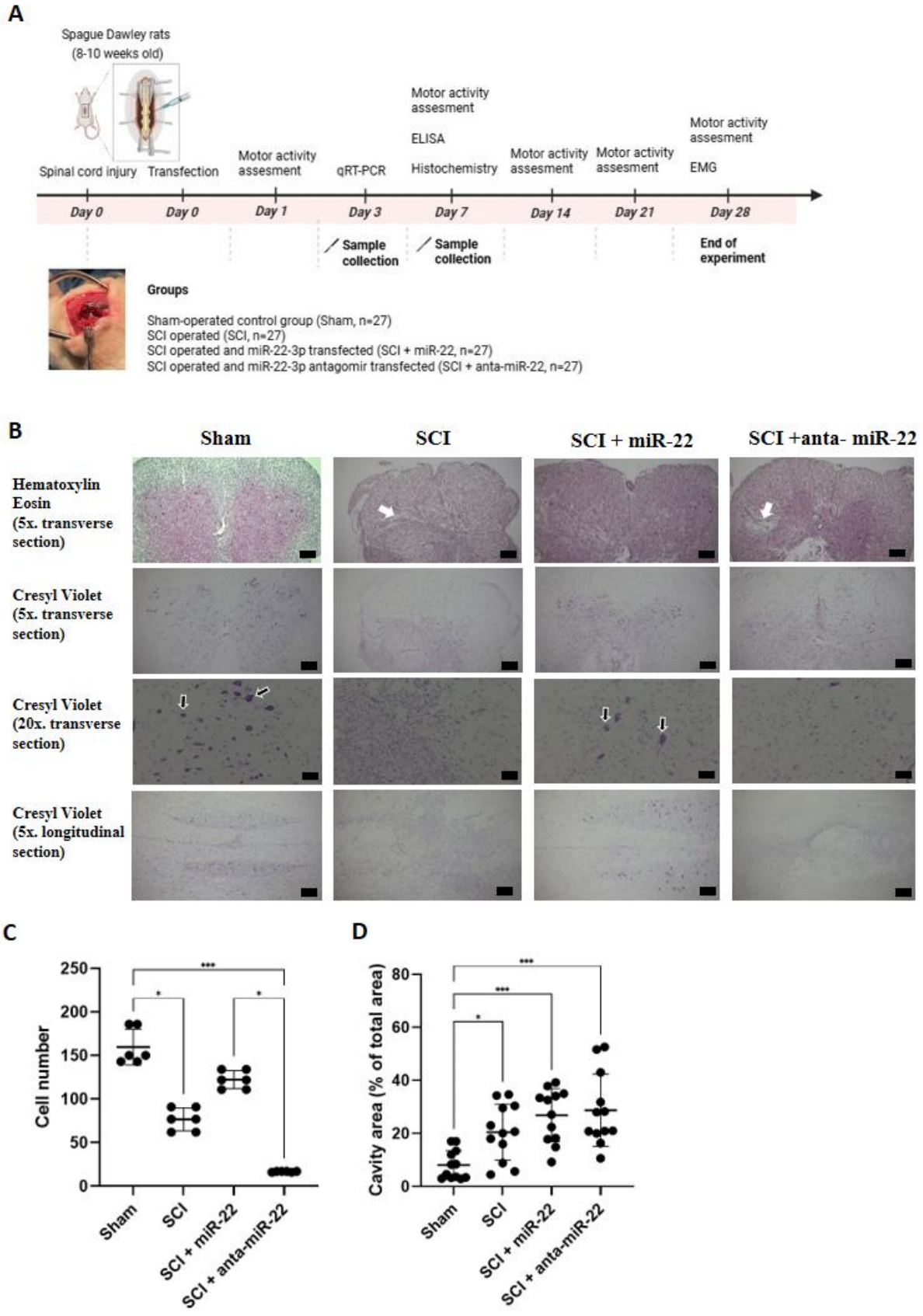


Fig. 1 Experimental design of the study (A). Histograms belongs to Hematoxylin eosin (HE) and Nissl staining of the spinal cord in different groups on day 7 (B). White arrows indicate

cavity areas and black arrows indicates Nissl positive neuron cells. Scale bars represent 100 μm (5×) and 400 μm (20×). Scatter plot graphics belong to analysis of cell count (n=6) (C) and cavity area (% of total area) (n=12) (D) after Nissl staining of sagittal sections of the spinal cord taken on day 7 post-surgery are presented (*p<0.05, ***p<0.001, ****p<0.0001).

The cell death marker expressions in the miR-22–transfected animals were less than in the SCI group

To evaluate the effects of miR-22 transfection on cell death–related pathways following SCI, the expression levels of cell death markers Bcl-2 and Caspase-3, and gliosis-associated marker GFAP were analyzed in spinal cord tissues. The expression of the anti-cell death marker Bcl-2 in the spinal cord tissues of the Sham group were found to be lower than in the SCI (p<0.0001), SCI + miR-22 (p=0.0497) and SCI + anta-miR-22 groups (p<0.0001) (Fig. 2A). Bcl-2 expression in the spinal cord tissues of the SCI + miR-22 group were found to be lower than in the SCI (p<0.0001) and SCI + anta-miR-22 groups (p<0.0001) (Fig. 2A). The expression of the anti-death marker Caspase-3 in the spinal cord tissues of the Sham group were found to be lower than in the SCI (p<0.0001) and SCI + anta-miR-22 groups (p<0.0001) (Fig. 2A). Caspase-3 expression in the spinal cord tissues of the SCI + miR-22 group were found to be lower than in the SCI (p<0.0001) and SCI + anta-miR-22 groups (p<0.0001) (Fig. 2A). In addition, GFAP levels in the spinal cord tissues of the Sham group were significantly lower compared to those in the SCI (p<0.0001), SCI + miR-22 (p<0.0001), and SCI + anta-miR-22 groups (p<0.0001) (Fig. 2A).

miR-22 expression was lower in spinal cord tissues of SCI group animals than that in Sham group

To evaluate the effect of miR-22 modulation on spinal cord injury, miR-22-3p expression levels were assessed in spinal cord tissues. miR-22-3p expression in SCI ($p=0.0001$), SCI + miR-22 ($p<0.0001$) and SCI + anta-miR-22 ($p<0.0001$) groups spinal cord tissues was significantly lower than that in spinal cord tissues obtained from the Sham group (Fig. 2B). Moreover, because of the transfection, miR-22-3p expression in the SCI + miR-22 group was significantly higher compared to SCI ($p<0.0001$), and SCI + anta-miR-22 groups ($p<0.0001$) (Fig. 2B).

The expressions of PTEN, STAT3, and CREB1 were lower in the spinal cord tissues of the miR-22-transfected group compared to those in the SCI group

To explore the molecular mechanisms underlying the effects of miR-22 transfection after spinal cord injury, PTEN, STAT3, CREB1, and AKT expression levels were evaluated in spinal cord tissues. PTEN expression was significantly higher in the spinal cord tissues of SCI ($p<0.0001$), SCI + miR-22 ($p<0.0001$), and SCI + anta-miR-22 ($p<0.0001$) groups compared with Sham group (Fig. 2C). PTEN expression in the SCI + miR-22 group was significantly lower than that in the SCI ($p<0.0001$) and SCI + anta-miR-22 ($p<0.0001$) groups (Fig. 2C). PTEN expression in the SCI + anta-miR-22 group was significantly lower than that in the SCI group ($p<0.0001$) (Fig. 2C). STAT3 expression in Sham group tissues was significantly lower compared to the SCI ($p<0.0001$) and SCI + anta-miR-22 ($p=0.0375$) group tissues (Fig. 2C). STAT3 expression in the SCI group tissues was significantly higher compared to the SCI + miR-22 ($p<0.0001$) and SCI + anta-miR-22 group ($p<0.0001$) tissues (Fig. 2C). No significant differences were observed among the groups in terms of AKT expression ($p>0.05$) (Fig. 2C). Compared with Sham group, CREB1 expression was significantly higher in the spinal cord tissues of SCI ($p<0.0001$), SCI + miR-22 ($p<0.0001$), and SCI + anta-miR-22 ($p<0.0001$) groups (Fig. 2C). CREB1 expression in the SCI group was significantly higher than that in the SCI + miR-22 ($p<0.0001$) and SCI + anta-miR-22 ($p=0.0004$) groups (Fig. 2C). In the SCI + miR-22 group,

CREB1 expression was lower compared to the SCI ($p<0.0001$), SCI + anta-miR-22 ($p<0.0001$) groups (Fig. 2C).

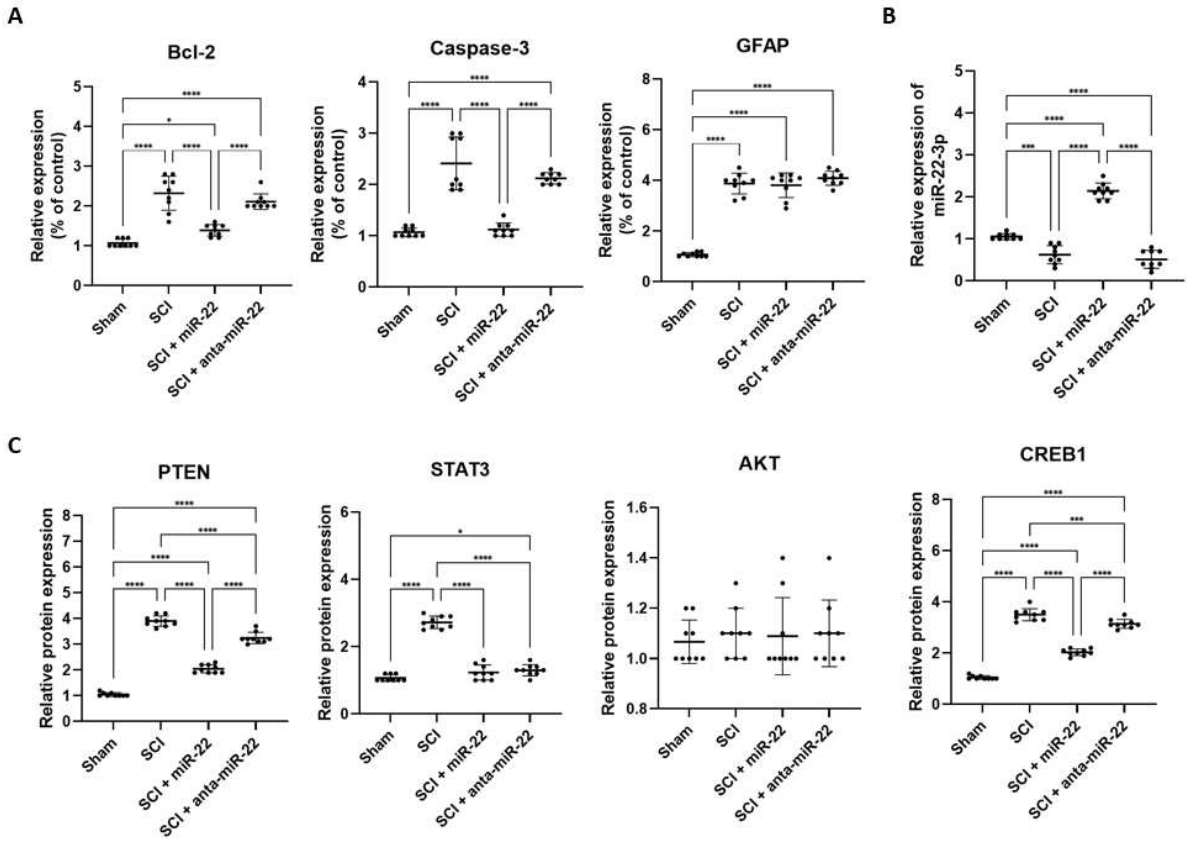


Fig. 2 mRNA and protein expression analysis. Expressions of Bcl-2 and Caspase-3 and astrocyte marker GFAP proteins on day 7 post-surgery are presented (A). mRNA expressions of miR-22-3p (B), PTEN, STAT3, AKT and CREB1 (C) on day 3 post-surgery are presented (n=9) (*$p<0.05$, **$p<0.01$, ***$p<0.001$, ****$p<0.0001$).

miR-22 transfection led to an increase in body weight at day 28 in animals subjected to SCI

Body weight changes were monitored over time to evaluate the effect of miR-22 transfection in animals subjected to SCI. The weight of sham rats increased on days 14 ($p=0.0491$), 21 ($p=0.0037$), and 28 ($p=0.0003$) compared to day 1 (Fig. 3A). The weight of sham rats increased

on days 21 (p=0.0026) and 28 (p=0.0042) compared to day 7 (Fig. 3A). The weight of sham rats increased on day 21 (p=0.0376) and 28 (p=0.0100) compared to day 14 (Fig. 3A). There were no significant differences in body weight among the rats in the SCI group across different days ($p > 0.05$) (Fig. 3A). The weight of SCI + miR-22 group rats increased on day 28 compared to day 14 (p=0.0047) (Fig. 3A). The weight of SCI + anta-miR-22 rats decreased on days 14 (p=0.0187), 21 (p=0.0340), and 28 (p=0.0128) compared to day 1 (Fig. 3A). When days were evaluated individually, on day 1, the weight of SCI (p=0.0352) and SCI + miR-22 (p=0.0427) group rats decreased compared to Sham group rats' (Fig. S1A). The weight of Sham group rats increased compared to SCI [p=0.0042 for day 7; p=0.0003 for day14; p=0.0002 for day 21; $p<0.0001$ for day 28], SCI + miR-22 [p=0.0114 for day 7; p=0.0025 for day14; p=0.0017 for day 21; p=0.0002 for day 28] and SCI + anta-miR-22 [p=0.0226 for day 7; p=0.0014 for day14; p=0.0004 for day 21; $p<0.0001$ for day 28] group rats on day 7, 14, 21 and 28 (Fig. S1A).

miR-22–transfected animals show significantly higher falling angles on day 28

The inclined plane test was performed to evaluate the effects of miR-22 transfection on motor function and balance following SCI. Sham, SCI and SCI + anta-miR-22 group animals exhibited falls at the same angles across all time points within their respective groups ($p > 0.05$) (Fig. 3B; Table S2). Rats transfected with miR-22 exhibited falls at greater angles on days 14 (p=0.0445) and 28 (p=0.0199) compared to day 1 (Fig. 3B; Table S2). When days were evaluated individually, SCI + anta-miR-22 group rats exhibited falls at smaller angles compared to Sham group on day 1 (p=0.0010) (Fig. S1B; Table S3). Falling angles of SCI [p=0.0069 for day 7; p=0.0013 for day 14; p=0.0013 for day 21; p=0.0011 for day 28] and SCI + anta-miR-22 [p=0.0007 for day 7; p=0.0016 for day 14; p=0.0015 for day 21; p=0.0017 for day 28] group rats exhibited falls at smaller angles compared to Sham group on days 7, 14, 21 and 28 (Fig.

S1B; Table S3). There were no significant differences in the falling angles between sham and miR-22–transfected rats at any time point ($p > 0.05$) (Fig. S1B; Table S3).

The motor activity of miR-22–transfected animals were significantly higher on day 28 compared to day 1

Longitudinal changes in motor activity were analyzed across experimental groups using the Drummond–Moore motor activity test with 22 criteria. Sham group animals exhibited same motor activity across all time points ($p > 0.05$) (Fig. 3C; Table S2). Motor activity of SCI group rats were significantly higher on day 28 compared to day 1 ($p=0.0071$) (Fig. 3C; Table S2). Motor activity of SCI + miR-22 group rats were significantly higher on day 21 ($p=0.0499$) and 28 ($p=0.0003$) compared to day 1 and on day 28 compared to day 7 ($p=0.0425$) (Fig. 3C; Table S2). Motor activity of SCI + anta-miR-22 group rats were significantly higher on day 28 compared to day 1 ($p=0.0088$) and 7 ($p=0.0088$) (Fig. 3C; Table S2). When days were evaluated individually, SCI [$p=0.0097$ for day 1; $p=0.0036$ for day 7; $p=0.0030$ for day 14; $p<0.0001$ for day 21; $p=0.0016$ for day 28] and SCI + anta-miR-22 [$p=0.0185$ for day 1, $p=0.0097$ for day 7; $p=0.0092$ for day 14; $p=0.0268$ for day 21; $p=0.0067$ for day 28] group rats exhibited lower motor activity compared to Sham group on days 1, 7, 14, 21 and 28 (Fig. S1C; Table S3). SCI + miR-22 group rats exhibited lower motor activity compared to Sham group only on days 1 ($p=0.0097$) (Fig. S1C; Table S3).

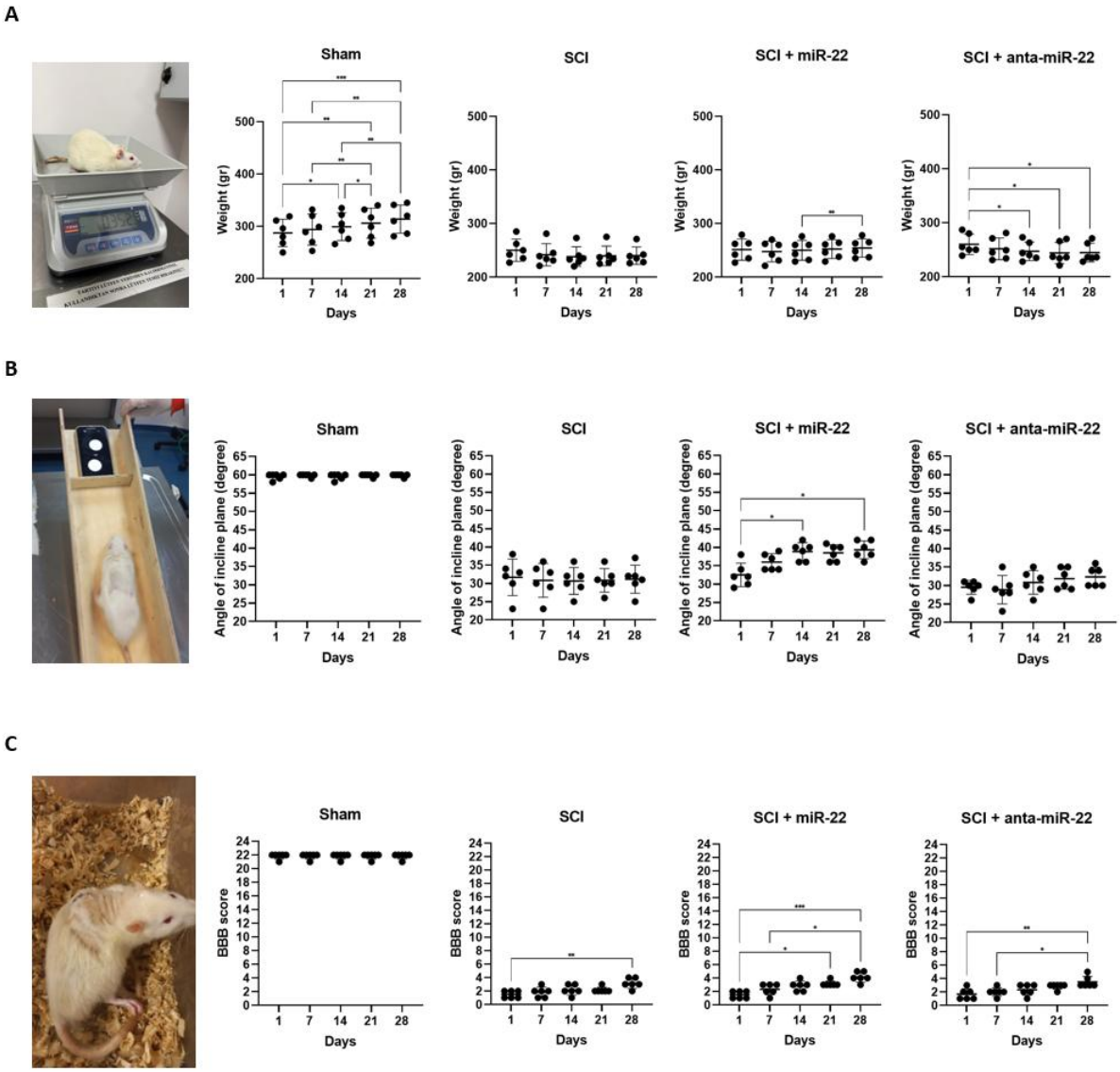


Fig 3. The results of weight measurements (A), the inclined plane test (B), and BBB motor activity test with 22 criteria (C) for all rats in the group were analyzed on the days 1, 7, 14, 21 and 28 (n=6) (*p<0.05, **p<0.01, ***p<0.001).

Step width measurements of miR-22–transfected animals were significantly higher on day 28 compared to day 1

Footprint analysis (Fig. 4A) was performed to evaluate step length, step width, and toe spread measurements (Fig. 4B) as indicators of locomotor function over time. Sham, SCI and SCI + anta-miR-22 group animals exhibited same step width measurements across all time points (p

> 0.05) (Fig. 4C). Step width measurements of SCI + miR-22 group rats were significantly lower on day 7 (p=0.0077), 14 (p=0.0038), 21 (p=0.0003), and 28 (p=0.0012) compared to day 1 (Fig. 4C). Step width measurements of SCI + miR-22 group rats were significantly higher on day 14 (p=0.0049), 21 (p=0.0003), and 28 (p=0.0011) compared to day 7 (Fig. 4C). Step width measurements of SCI + miR-22 group rats were significantly higher on day 21 (p=0.0109), and 28 (p=0.0074) compared to day 14 (Fig. 4C). When days were evaluated individually, SCI (p<0,0001 for day 1, 7, 14, 21, and 28), SCI + miR-22 (p<0,0001 for day 1, 7, 14, 21, and 28), and SCI + anta-miR-22 (p<0,0001 for day 1, 7, 14, 21, and 28) group rats exhibited higher step width measurements compared to Sham group on days 1, 7, 14, 21 and 28 (Fig. S2A). SCI (p=0.0004 for day 14; p<0,0001 for day 21 and 28), and SCI + anta-miR-22 (p=0.0030 for day 14; p<0,0001 for day 21 and 28) group rats exhibited higher step width measurements compared to SCI + miR-22 on days 14, 21 and 28 (Fig. S2A).

Step length measurements of miR-22–transfected animals were significantly higher on day 28 compared to day 1

When step length was analyzed, Sham and SCI + anta-miR-22 group animals exhibited similar step length measurements across all time points (p>0.05) (Fig. 4D). Step length measurements of SCI group rats were significantly higher on day 7 compared to day 21 (p=0.0492) (Fig. 4D). Step length measurements of SCI + miR-22 group rats were significantly lower on day 21 (p=0.0410) and 28 (p=0.0248) compared to day 1 (Fig. 4D). When days were evaluated individually, SCI (p<0,0001 for day 1, 7, 14, 21, and 28), SCI + miR-22 (p<0,0001 for day 1, 7, 14, 21, and 28), and SCI + anta-miR-22 (p<0,0001 for day 1, 7, 14, 21, and 28) group rats exhibited higher step length measurements compared to Sham group on days 1, 7, 14, 21 and 28 (Fig. S2B). SCI + anta-miR-22 group rats exhibited higher step width measurements compared to SCI + miR-22 on day 1 (p=0.0079) (Fig. S2B). SCI [p=0.0072 for day 7; p=0.0007

for day 14; p=0.0018 for day 21; p=0.0014 for day 28], and SCI + anta-miR-22 [p=0.0008 for day 7; p=0.0002 for day 14; p=0.70002 for day 21; p=0.0002 for day 28] group rats exhibited higher step width measurements compared to SCI + miR-22 on days 7, 14, 21 and 28 (Fig. S2B).

Toe spread recovery was not observed in the miR-22–transfected animals

When toe spread was analyzed, Sham, SCI, SCI + miR-22, and SCI + anta-miR-22 group animals exhibited similar toe spread measurements across all time points ($p > 0.05$) (Fig. 4E). When days were evaluated individually, SCI ($p<0,0001$ for day 1, 7, 14, 21, and 28), SCI + miR-22 (p=0.0001 for day 1; p=0.0060 for day 7; p=0.0020 for day 14; p=0.0035 for day 21; p=0.0129 for day 28), and SCI + anta-miR-22 ($p<0,0001$ for day 1, 7, 14, 21, and 28) group rats exhibited lower toe spread measurements compared to Sham group on days 1, 7, 14, 21 and 28 (Fig. S2B). SCI (p=0.0019 for day 1; p=0.0015 for day 7; p=0.0198 for day 14; p=0.0093 for day 21; p=0.0258 for day 28) and SCI + anta-miR-22 (p=0.0152 for day 1; p=0.0109 for day 7; p=0.0487 for day 14; p=0.0163 for day 21; p=0.0129 for day 28) group rats exhibited lower toe spread measurements compared to SCI + miR-22 on days 1, 7, 14, 21, and 28 (Fig. S2B).

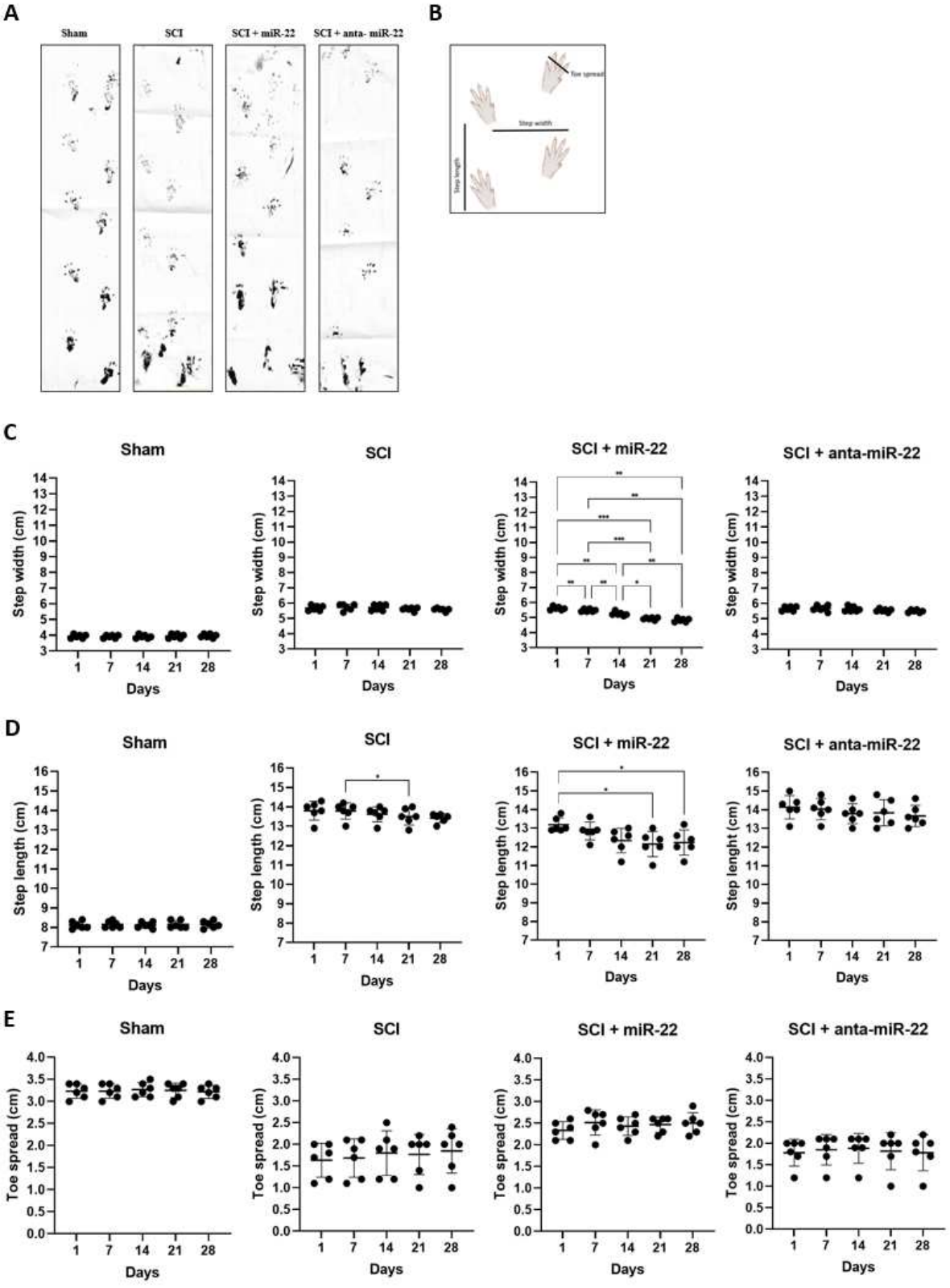


Fig. 4 Representative footprint analysis of Sham, SCI, SCI + miR-22, and SCI + anta-miR-22 groups (A). Schematic used for quantifying step width, step length and toe spread (B). Graphs

belongs to analysis of step width (C), step length (D) and toe spread (E) on days 1, 7 ,14, 21 and 28 (n=6) (*p<0.05, **p<0.01, ***p<0.001).

The proximal latency of miR-22 transfected animals was better than those of SCI group animals

To assess the effects of miR-22 transfection on peripheral nerve function, compound muscle action potential (CMAP) parameters were analyzed on day 28 (Fig. 5A). Proximal latency of SCI (p=0.0004) and SCI + anta-miR-22 (p=0.0003) group animals appeared higher compared to Sham group animals (Fig. 5B). Proximal latency of SCI (p=0.0072) and SCI + anta-miR-22 (p=0.0057) group animals was higher compared to SCI + miR-22 group animals (Fig. 5B). Proximal amplitude was higher in Sham group animals compared to the SCI (p<0.0001), SCI + miR-22 (p<0.0001), and SCI + anta-miR-22 (p<0.0001) groups (Fig. 5C). Conduction velocity was higher in Sham group animals compared to the SCI (p<0.0001), SCI + miR-22 (p<0.0001), and SCI + anta-miR-22 (p<0.0001) groups (Fig. 5D). Conduction block of SCI (p<0.0001), SCI + miR-22 (p<0.0001) and SCI + anta-miR-22 (p<0.0001) group animals was higher compared to Sham group animals (Fig. 5E). CMAP duration of SCI (p=0.0158) and SCI + anta-miR-22 (p=0.0104) group animals was higher compared to Sham group animals (Fig. 5F). SCI + anta-miR-22 group rats exhibited higher CMAP duration compared to SCI + miR-22 (p=0.0401) (Fig. 5F).

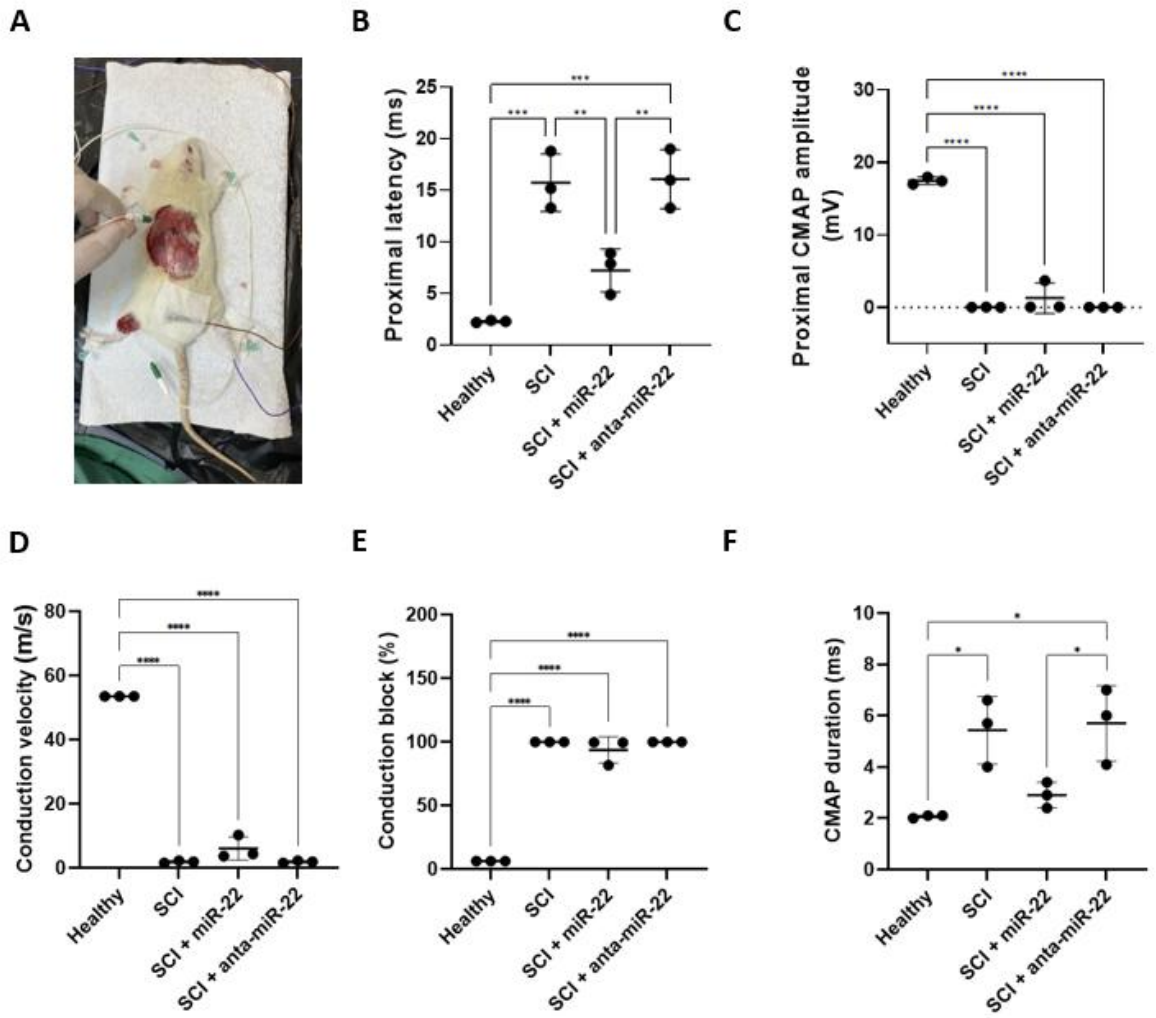


Fig. 5 Representative EMG analysis of a rat (A). Graphs belongs to analysis of proximal latency (ms) (B), proximal CMAP amplitude (mV) (C), conduction velocity (m/s) (D), conduction block (%) (E), and CMAP duration (ms) (F) on day 28 (n=3) (*p<0.05, **p<0.01, ***p<0.001, ****p<0.0001). CMAP: compound muscle action potential

Discussion

In our study, miR-22 expression was found to be reduced in the injured spinal cord tissues of rats following SCI, a finding consistent with some previous reports. Although, miR-22 has been previously reported in the brain [8-10], where it is localized to both neurons and glial cells [11], its role in the spinal cord is less defined. Our results confirm its presence in spinal cord tissue and demonstrate a significant decrease after injury. For instance, one study using a traumatic

SCI mouse model reported an approximate twofold decrease in miR-22 levels on days 1 and 3 post-injury [25]. In our model, we successfully increased miR-22 expression in injured tissues by approximately twofold through transient transfection. The limited magnitude of this increase is likely attributable to the transient nature of the transfection strategy and the fact that expression was evaluated on day 3 post-injury.

Histological analyses on day 7 post-injury revealed a higher neuronal cell count in the spinal cord tissues of the miR-22–transfected group compared to injured control and also there is no significant difference between sham control. This neuroprotective effect is consistent with the established role of miR-22 as a potent antioxidant and anti-inflammatory agent [6, 7]. The literature indicates that miR-22 exerts anti-apoptotic effects by modulating key pathways, such as suppressing the Bax/Bcl-2 and cleaved caspase-3/caspase-9 ratios in rat myoblasts [7]. Furthermore, studies show that mesenchymal stem cell (MSC) derived extracellular vesicle (EV) loaded with miRNA- 22 can inhibit the post-SCI inflammatory response by reducing levels of IL-1β, IL-18 and TNF, while also decreasing scar formation [25]. Collectively, these findings indicate that miR-22 protects cells from disease and injury through its antioxidative, anti-inflammatory, and cell survival effects [6, 7, 25]. In our study, however, the observed neuroprotection was not accompanied by a reduction in cavity volume. This discrepancy may be attributed to miR-22-enhanced glial proliferation contributing to glial scar formation [26], or it may simple reflect that the assessment at day 7 captured an early phase of the regenerative process, before significant tissue remodeling could occur [27]. Nonetheless, in line with the mechanisms described above, our findings demonstrate that miR-22 overexpression following SCI can effectively prevent neuronal cell loss in the injured spinal cord.

Transfection with miR-22 reduced the levels of the cell death markers Caspase-3 and Bcl-2 compared to the injured control and also there is no significant difference between sham control, suggesting a protective role for miR-22 through the attenuation of cell death. This finding aligns

with previous studies. The decrease in Caspase-3 following miR-22 transfection has been reported not only in rat models of spinal cord injury [17] but also in human umbilical vein endothelial cells (HUVECs) [28] and myocardial infarction models [29]. This indicates that the anti-cell death effect of miR-22 may be a broader regulatory mechanism common to various pathologies. Similarly, reduced Bcl-2 levels after miR-22 transfection have been observed in rat models of spinal cord injury models [30], rat myoblasts [7], and gastrointestinal stromal tumor cell lines [31]. Together, these findings suggest that miR-22 modulates cell death-related pathways, and its regulation of Bcl-2 and Caspase-3 likely contributes to tissue repair and functional recovery following SCI. These molecular results are further supported by our histological data, which showed a decrease in death cells following miR-22 transfection.

In our study, the level of GFAP protein-a well-established marker of astrocytic activation and neural tissue repair-was increased in injured tissues compared to uninjured controls [32]. However, in our study, transfection with either miR-22 or anta-miR-22 did not significantly alter GFAP levels relative to the SCI-only group. These findings suggest that miR-22 may not directly regulate astrocytic activation following SCI, despite its influence on other cell death and signaling pathways. To the best of our knowledge, no prior studies have specifically investigated the relationship between miR-22 and GFAP expression in the context of SCI. The only relevant evidence comes from a study demonstrating that GFAP levels remained unchanged in both epileptic and sham miR-22 knockout mice [33], further supporting the possibility that miR-22 does not substantially modulate GFAP expression under pathological conditions.

In the present study, PTEN mRNA levels in the spinal cord tissues were reduced in the miR-22–transfected group compared to the injured control, whereas AKT mRNA expression did not show a significant change. PTEN is a well-established negative regulator of the PI3K/AKT pathway; however, its regulatory role primarily affects AKT phosphorylation rather than

transcriptional regulation [34]. Therefore, the absence of changes in AKT mRNA levels in our study does not exclude alterations in AKT activity [34]. A limitation of the present study is that phosphorylated AKT (p-AKT) levels were not assessed, and thus potential changes in AKT activation cannot be determined. It is possible that PTEN downregulation observed at day 3 may be associated with delayed or transient changes in AKT signaling at later time points. In addition, injured neural tissue may maintain AKT activity through compensatory mechanisms involving alternative signaling pathways, such as MAPK/ERK [34]. Previous studies have reported that modulation of PTEN activity is associated with axonal growth and functional recovery following spinal cord injury [13, 14]; however, further mechanistic investigations are required to clarify whether similar pathways are involved under the experimental conditions of the present study.

In the present study, STAT3 mRNA expression was reduced following both miR-22 mimic and miR-22 antagomir transfection. This observation suggests that changes in STAT3 expression are not specifically dependent on the direction of miR-22 modulation under the experimental conditions used. With respect to CREB1, its expression in the miR-22–transfected group was higher than in the uninjured control but lower than in the injured control, indicating a context-dependent pattern of regulation. This observation is consistent with previous findings demonstrating miR-22–3p–mediated downregulation of CREB1 in human renal cell carcinoma cell lines [35]. Collectively, these results suggest that miR-22 may be associated with context-dependent modulation of CREB1 expression; however, the functional relevance of these changes for neuronal survival or regeneration requires further investigation.

Following miR-22 transfection, rat weights increased on day 28 compared to day 14, in contrast to the SCI group, in which no increase was observed. Considering the decrease in body weight observed in the SCI group and the increase in body weight in Sham group, miR-22 transfection may contribute to an improvement in overall animal health. BBB, inclined plane test, footprint

test demonstrated significant improvements in the miR-22 transfected groups compared to injured controls. These functional improvements were partially supported by electrophysiological evaluations (just in proximal latency). In the previous study, the latency of miRNA-22 loaded MSC derived EV application in SCI model rats was found shorter than in the SCI group, but not different from the EV group on day 15 [25]. Similarly, in our study, proximal latency was shorter in miR-22 transfected rats compared to the SCI group. Furthermore, no difference was found between Sham and miR-22 group in CMAP duration on day 28. However, miR-22 transfection did not lead to improvements in proximal amplitude, conduction velocity, and conduction block. This discrepancy may be attributed to compensatory mechanisms and neuroplasticity, which can enhance motor performance without complete restoration of axonal conduction [36, 37]. Furthermore, miR-22 may promote neuronal survival and local circuit reorganization rather than full long-distance axonal regeneration, which could explain the absence of measurable electrophysiological recovery [36]. It is also possible that the evaluation period was too early for detectable electrophysiological improvement, as remyelination and synaptic reconnection typically occur later in the repair process or glial scar [36, 37].

Conclusions

Our study demonstrates that miR-22 transfection in rats with SCI promoted neuronal regeneration and functional recovery. The treatment led to an increased neuronal cell count, decreased PTEN and STAT3 levels, elevated GFAP protein, a reduction in the cell death markers Bcl-2 and Caspase-3, and improved motor function. However, several limitations should be acknowledged. The transient nature of the transfection and the reliance on single time-point analyses may not fully capture the temporal dynamics of miR-22-mediated effects. Furthermore, the electrophysiological findings should be interpreted with caution, as the analysis was performed using a limited number of biological replicates. Therefore, these

findings should be considered preliminary and exploratory and warrant confirmation in studies with larger sample sizes. While these findings present a novel contribution to the literature, they require confirmation through replication and alternative methodologies. Future studies employing sustained miR-22 delivery systems and combinatorial therapeutic approaches are warranted to further elucidate and enhance the reparative potential after SCI.

Acknowledgements Studies were carried out using equipment of the Akdeniz University, Prof. Dr. Tuncer Karpuzoğlu Research Center and Akdeniz University, Animal Care Unit.

Author Contributions S.K., Öm.Ö., and Öz.Ö. are the authors of the main idea of the article. S.K., S.T., Öm.Ö., and Öz.Ö. conducted the in vivo model creation and experiments. S.K., O.T., and E.A.D. conducted the EMG experiments. S.K., Öm.Ö., and Öz.Ö performed all other experiments and analyses. All authors reviewed the manuscript.

Funding This work was supported by Scientific Research Coordination Unit of Akdeniz University (#TSA-2023-6511).

Declarations

Competing Interests The authors have no relevant financial or non-financial interests to disclose.

Ethical Approval All animal experiments were performed in accordance with the National Institutes of Health (NIH) Guide for the Care and Use of Laboratory Animals and were approved by the Animal Care and Use Committee of the Akdeniz University (#1564/2023.05.002).

Data Availability

All data generated or analyzed during this study are included in this published article and its supplementary information files.

References

1. O'Shea TM, Burda JE, Sofroniew MV. Cell biology of spinal cord injury and repair. J Clin Invest. 2017;127(9):3259-70. doi: 10.1172/JCI90608.

2. Jazayeri SB, Beygi S, Shokraneh F, Hagen EM, Rahimi-Movaghar V. Incidence of traumatic spinal cord injury worldwide: a systematic review. Eur Spine J. 2015;24(5):905-18. doi: 10.1007/s00586-014-3424-6.

3. Alizadeh A, Dyck SM, Karimi-Abdolrezaee S. Traumatic Spinal Cord Injury: An Overview of Pathophysiology, Models and Acute Injury Mechanisms. Front Neurol. 2019;10:282. doi: 10.3389/fneur.2019.00282.

4. Ghibaudi M, Boido M, Vercelli A. Functional integration of complex miRNA networks in central and peripheral lesion and axonal regeneration. Prog Neurobiol. 2017;158:69-93. doi: 10.1016/j.pneurobio.2017.07.005.

5. Silvestro S, Mazzon E. MiRNAs as Promising Translational Strategies for Neuronal Repair and Regeneration in Spinal Cord Injury. Cells. 2022;11(14). doi: 10.3390/cells11142177.

6. Dong H, Cui B, Hao X. MicroRNA-22 alleviates inflammation in ischemic stroke via p38 MAPK pathways. Mol Med Rep. 2019;20(1):735-44. doi: 10.3892/mmr.2019.10269.

7. Tang Q, Len Q, Liu Z, Wang W. Overexpression of miR-22 attenuates oxidative stress injury in diabetic cardiomyopathy via Sirt 1. Cardiovasc Ther. 2018;36(2). doi: 10.1111/1755-5922.12318.

8. Cao Y, Liu H, Zhang J, Dong Y. Circular RNA cZNF292 silence alleviates OGD/R-induced injury through up-regulation of miR-22 in rat neural stem cells (NSCs). Artif Cells Nanomed Biotechnol. 2020;48(1):594-601. doi: 10.1080/21691401.2020.1725536.

9. Hu J, Zhou W, Zhou Z, Yang Q, Xu J, Dong W. miR-22 and cerebral microbleeds in brainstem and deep area are associated with depression one month after ischemic stroke. Braz J Med Biol Res. 2020;53(5):e9162. doi: 10.1590/1414-431x20209162.

10. Wang X, Shi C, Pan H, Meng X, Ji F. MicroRNA-22 exerts its neuroprotective and angiogenic functions via regulating PI3K/Akt signaling pathway in cerebral ischemia-reperfusion rats. J Neural Transm (Vienna). 2020;127(1):35-44. doi: 10.1007/s00702-019-02124-7.

11. Jimenez-Mateos EM, Arribas-Blazquez M, Sanz-Rodriguez A, Concannon C, Olivos-Ore LA, Reschke CR, et al. microRNA targeting of the P2X7 purinoceptor opposes a contralateral epileptogenic focus in the hippocampus. Sci Rep. 2015;5:17486. doi: 10.1038/srep17486.

12. Wang W, Su Y, Tang S, Li H, Xie W, Chen J, et al. Identification of noncoding RNA expression profiles and regulatory interaction networks following traumatic spinal cord injury by sequence analysis. Aging (Albany NY). 2019;11(8):2352-68. doi: 10.18632/aging.101919.

13. Park KK, Liu K, Hu Y, Smith PD, Wang C, Cai B, et al. Promoting axon regeneration in the adult CNS by modulation of the PTEN/mTOR pathway. Science. 2008;322(5903):963-6. doi: 10.1126/science.1161566.

14. Sun F, Park KK, Belin S, Wang D, Lu T, Chen G, et al. Sustained axon regeneration induced by co-deletion of PTEN and SOCS3. Nature. 2011;480(7377):372-5. doi: 10.1038/nature10594.

15. Percie du Sert N, Hurst V, Ahluwalia A, Alam S, Avey MT, Baker M, et al. The ARRIVE guidelines 2.0: Updated guidelines for reporting animal research. J Cereb Blood Flow Metab. 2020;40(9):1769-77. doi: 10.1177/0271678X20943823.

16. Wang T, Li B, Yuan X, Cui L, Wang Z, Zhang Y, et al. MiR-20a Plays a Key Regulatory Role in the Repair of Spinal Cord Dorsal Column Lesion via PDZ-RhoGEF/RhoA/GAP43 Axis in Rat. Cell Mol Neurobiol. 2019;39(1):87-98. doi: 10.1007/s10571-018-0635-0.

17. Li B, Wang Z, Yu M, Wang X, Wang X, Chen C, et al. miR-22-3p enhances the intrinsic regenerative abilities of primary sensory neurons via the CBL/p-EGFR/p-STAT3/GAP43/p-GAP43 axis. J Cell Physiol. 2020;235(5):4605-17. doi: 10.1002/jcp.29338.

18. Poongodi R, Yang TH, Huang YH, Yang KD, Chen HZ, Chu TY, et al. Stem cell exosome-loaded Gelfoam improves locomotor dysfunction and neuropathic pain in a rat model of spinal cord injury. Stem Cell Res Ther. 2024;15(1):143. doi: 10.1186/s13287-024-03758-5.

19. Yu M, Wang F, Han K. Silencing of SH3BP2 Inhibits Microglia Activation Via the JAK/STAT Signaling in Spinal Cord Injury Models. Inflammation. 2025;48(4):2230-43. doi: 10.1007/s10753-024-02186-0.

20. Zarei-Kheirabadi M, Hesaraki M, Kiani S, Baharvand H. In vivo conversion of rat astrocytes into neuronal cells through neural stem cells in injured spinal cord with a single zinc-finger transcription factor. Stem Cell Res Ther. 2019;10(1):380. doi: 10.1186/s13287-019-1448-x.

21. Yu T, Zhao C, Hou S, Zhou W, Wang B, Chen Y. Exosomes secreted from miRNA-29b-modified mesenchymal stem cells repaired spinal cord injury in rats. Braz J Med Biol Res. 2019;52(12):e8735. doi: 10.1590/1414-431X20198735.

22. Chen L, Li X, Zhu J, Xu B, Gu Y. miRNA-19a exerts an anti-apoptotic effect in spinal cord injured rats via the PTEN pathway. Arch Med Sci. 2023;19(3):744-56. doi: 10.5114/aoms.2019.90008.

23. Kose S, Aerts-Kaya F, Kopru CZ, Nemutlu E, Kuskonmaz B, Karaosmanoglu B, et al. Human bone marrow mesenchymal stem cells secrete endocannabinoids that stimulate in vitro hematopoietic stem cell migration effectively comparable to beta-adrenergic stimulation. Exp Hematol. 2018;57:30-41 e1. doi: 10.1016/j.exphem.2017.09.009.

24. Aerts-Kaya F, Kilic E, Kose S, Aydin G, Cagnan I, Kuskonmaz B, et al. G-CSF treatment of healthy pediatric donors affects their hematopoietic microenvironment through changes in bone marrow plasma cytokines and stromal cells. Cytokine. 2021;139:155407. doi: 10.1016/j.cyto.2020.155407.

25. Sheng Y, Zhou X, Wang J, Shen H, Wu S, Guo W, et al. MSC derived EV loaded with miRNA-22 inhibits the inflammatory response and nerve function recovery after spinal cord injury in rats. J Cell Mol Med. 2021;25(21):10268-78. doi: 10.1111/jcmm.16965.
26. Herrmann JE, Imura T, Song B, Qi J, Ao Y, Nguyen TK, et al. STAT3 is a critical regulator of astrogliosis and scar formation after spinal cord injury. J Neurosci. 2008;28(28):7231-43. doi: 10.1523/JNEUROSCI.1709-08.2008.
27. Hyun JK, Kim HW. Clinical and experimental advances in regeneration of spinal cord injury. J Tissue Eng. 2010;2010:650857. doi: 10.4061/2010/650857.
28. Xu D, Guo Y, Liu T, Li S, Sun Y. miR-22 contributes to endosulfan-induced endothelial dysfunction by targeting SRF in HUVECs. Toxicol Lett. 2017;269:33-40. doi: 10.1016/j.toxlet.2017.01.014.
29. Wang L, Wang L, Wang Q. Constitutive activation of the NEAT1/miR-22-3p/Ltb4r1 signaling pathway in mice with myocardial injury following acute myocardial infarction. Aging (Albany NY). 2021;13(11):15307-19. doi: 10.18632/aging.203089.
30. Li K, Liu Z, Wu P, Chen S, Wang M, Liu W, et al. Micro electrical fields induced MSC-sEVs attenuate neuronal cell apoptosis by activating autophagy via lncRNA MALAT1/miR-22-3p/SIRT1/AMPK axis in spinal cord injury. J Nanobiotechnology. 2023;21(1):451. doi: 10.1186/s12951-023-02217-2.
31. Xu Y, Cheng M, Mi L, Qiu Y, Hao W, Li L. Mir-22-3p Enhances the Chemosensitivity of Gastrointestinal Stromal Tumor Cell Lines to Cisplatin through PTEN/PI3K/Akt Pathway. Iran J Allergy Asthma Immunol. 2018;17(4):318-25. doi: 10.18502/ijaai.v17i4.91.
32. Brenner M. Role of GFAP in CNS injuries. Neurosci Lett. 2014;565:7-13. doi: 10.1016/j.neulet.2014.01.055.
33. Almeida Silva LF, Reschke CR, Nguyen NT, Langa E, Sanz-Rodriguez A, Gerbatin RR, et al. Genetic deletion of microRNA-22 blunts the inflammatory transcriptional response to

status epilepticus and exacerbates epilepsy in mice. Mol Brain. 2020;13(1):114. doi: 10.1186/s13041-020-00653-x.

34. Georgescu MM. PTEN Tumor Suppressor Network in PI3K-Akt Pathway Control. Genes Cancer. 2010;1(12):1170-7. doi: 10.1177/1947601911407325.

35. Friedrich M, Heimer N, Stoehr C, Steven A, Wach S, Taubert H, et al. CREB1 is affected by the microRNAs miR-22-3p, miR-26a-5p, miR-27a-3p, and miR-221-3p and correlates with adverse clinicopathological features in renal cell carcinoma. Sci Rep. 2020;10(1):6499. doi: 10.1038/s41598-020-63403-y.

36. Punjani N, Deska-Gauthier D, Hachem LD, Abramian M, Fehlings MG. Neuroplasticity and regeneration after spinal cord injury. N Am Spine Soc J. 2023;15:100235. doi: 10.1016/j.xnsj.2023.100235.

37. Curt A, Van Hedel HJ, Klaus D, Dietz V, Group E-SS. Recovery from a spinal cord injury: significance of compensation, neural plasticity, and repair. J Neurotrauma. 2008;25(6):677-85. doi: 10.1089/neu.2007.0468.

Supplementary Files

This is a list of supplementary files associated with this preprint. Click to download.

- TableS1.jpg
- TableS2.jpg
- TableS3.jpg
- Supplementaryfiguresandtables.docx
- Supplementarydata.xlsx
- Graphicalabstract.jpg